# Design of an Electro-Optic Modulator Based on a Silicon-Plasmonic Hybrid Phase Shifter

Mu Xu, Fei Li, Tao Wang, *Senior Member, IEEE*, Jiayang Wu, Liyang Lu, Linjie Zhou, *Member, IEEE*, and Yikai Su, *Senior Member, IEEE*

*Abstract*—We propose a silicon-compatible plasmonic electro-optic modulator employing a silicon racetrack ring resonator coupled to a bus waveguide. A silicon-plasmonic hybrid phase shifter clad with electro-optic polymer is introduced to achieve high-speed performance and low energy consumption. Simulations show that the proposed modulator can achieve an extinction ratio of more than 15 dB at 1550-nm wavelength under a 1.2-V bias voltage. The misalignment tolerance and fabrication feasibility of the modulator are also discussed.

*Index Terms*—Electro-optic modulators, plasmonics, racetrack ring resonators, silicon photonics.

## I. INTRODUCTION

**H**IGH speed modulation is an essential requirement in optical communication systems and short-reach optical interconnects. Due to its low cost and compatibility with the state-of-the-art complementary metal-oxide-semiconductor (CMOS) fabrication processes, silicon has already shown its potential in optical modulators with bandwidths of more than 30 GHz [1], relying on free carrier plasma dispersion (FCPD) effect induced by carrier accumulation, carrier injection, or carrier depletion [2].

However, the achievable bandwidths of FCPD based silicon modulators are limited by the time constants related to the free carrier injection and extraction [3], [4]. To overcome this limitation, hybrid silicon platforms have been suggested. By combining silicon strips with nonlinear electro-optic (EO) organic materials or high-absorption multilayer III–V quantum well materials, the modulation bandwidths can be increased to more than 40 GHz [3], [5]. Although the ultrafast $\chi^{(2)}$ nonlinear processes in organic materials show the prospect in realizing extremely high speed modulators, the bandwidths of the hybrid silicon modulators are still narrower than expected due to electrical properties, such as large resistance induced by doped silicon strips or contacts [6], and weak mode confinement that causes a considerable proportion of light localized in the silicon region.

Moreover, the effective index changes induced by FCPD are typically on the order of $10^{-4}$ to $10^{-3}$, thus requiring large footprints with long plate electrodes for Mach-Zehnder silicon modulators. There are three issues to address in designing silicon modulators with long parallel-plate electrodes. Firstly, the phase velocities of the electrical and optical waves ought to be matched. Secondly, the characteristic impedance of the phase shifter should be equal to that of the termination resistor in order to eliminate the back reflection on the transmission line. Thirdly, the transmission loss of both the electrodes and the optical waveguides should be small enough to maintain the extinction ratio under dynamic modulation. However, it is difficult to optimize all the three aspects simultaneously, thus imposing a limit on the bandwidths of silicon modulators [7]. On the other hand, although silicon ring or disk modulators have micron-sized footprints eliminating the need for travelling-wave design, the photon life times of the ring resonators set an additional fundamental limit to the modulation speed [8].

Recent progresses in plasmonic photonics lead to a great improvement in the optical-waveguide confinement capability and may provide a solution to the design of electro-optic modulator without using doped silicon to conduct electrical signals [9], [10]. However, the propagation length of the plasmonic mode is limited by the material loss in metal [11], which prevents plasmonic devices from large-scale integration. Plasmonic electro-absorption modulators have been fabricated based on modulating carrier density within metal-oxide and metal-oxide-semiconductor layered structures [12]–[15]. Several plasmonic electro-optic modulators have also been theoretically proposed [9], [16], [17]. Although compact, the modulators in [9], [16], and [17] suffer from high loss, low modulation efficiency or challenges in coupling and manufacturing processes.

In this work, we propose a silicon-plasmonic hybrid racetrack ring modulator having a compact size, a large modulation bandwidth, and relatively low power consumption. As shown in Fig. 1(a), the proposed modulator is based on a silicon racetrack ring resonator coupled to a bus waveguide. A metal-dielectric-metal (MDM) waveguide is positioned above one of the straight-waveguide sections of the racetrack ring with an insulating layer of silicon di-oxide. The slot of the MDM plasmonic waveguide is filled with EO polymer. The straight-waveguide section and the MDM plasmonic waveguide together act as a hybrid phase shifter where the signal voltage across the two parallel metal plates changes the refractive index of the

Fig. 1. (Color online) Structure of the silicon-compatible racetrack ring modulator. (a) Perspective view of the racetrack ring resonator with the MDM waveguide situated on top. (b) Perspective view of the silicon-plasmonic hybrid phase shifter. $l_{hp}$: length of the silicon-plasmonic hybrid phase shifter. $r$: radius of the racetrack ring. $H_{sp}$: height of the silica space between the silicon waveguide and the metal plates. $W_{si}$ and $H_{si}$: width and height of the silicon waveguide, respectively. $d$ and $H_{slot}$: width and height of the slot, respectively.

polymer filled in the slot through the Pockels effect, hence modulating the phase of the plasmonic wave guided in the MDM waveguide. Ignoring the electrical and structural limitations, the intrinsic modulation speed of EO polymer can be ultrafast [18]. By introducing the ring structure, the length of the silicon-plasmonic hybrid phase shifter can be shortened in comparison with that of a Mach-Zehnder interferometer or a single waveguide phase shifter. The proposed modulator can be directly integrated with the state-of-the-art silicon-on-insulator (SOI) photonic structures through the bus waveguide to form a compact electro-optical link.

## II. SILICON-COMPATIBLE HIGH-SPEED MODULATOR INTEGRATED WITH A SILICON-PLASMONIC HYBRID PHASE SHIFTER

### A. Structure of the Silicon-Plasmonic Hybrid Phase Shifter

The silicon-plasmonic hybrid phase shifter of the proposed modulator consists of two layers as shown in Fig. 1(b). The bottom layer comprises one single-mode silicon waveguide embedded in silicon di-oxide. The upper layer comprises two parallel symmetric metal (e.g. Ag) plates isolated by a 30-nm to
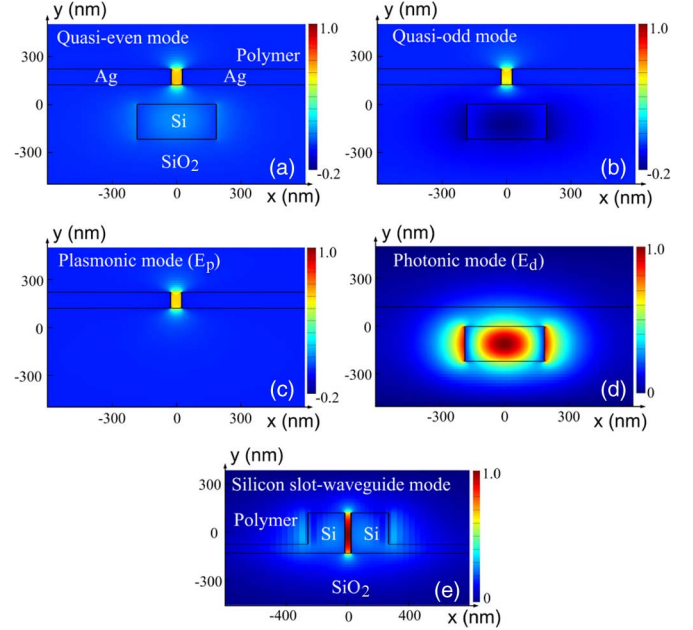


Fig. 2. (Color online) Electric field distributions ($E_x$) of (a) quasi-even mode and (b) quasi-odd mode supported by the silicon-plasmonic hybrid waveguide; (c) plasmonic mode supported by the MDM slotline; (d) photonic mode supported by the silicon strip waveguide; and (e) silicon slot-waveguide mode. All waveguides in (a), (b), (c), and (e) have 50-nm-wide slots filled with polymer ($n_p = 1.63$). The height of the MDM waveguide is 100 nm. The width and height of the silicon strip in (d) are 370 nm and 220 nm, respectively. The silicon slot-waveguide in (e) is composed of two 220-nm-high and 150-nm-wide silicon strips with 50-nm-thick silicon slabs extending to both sides.

80-nm wide gap and upper-clad with EO polymer to form an MDM structure. The metal plates are 100-nm-thick and extend to both sides for electrode contacts. The length of the phase shifter is determined by the coupling length between the fundamental modes of the MDM waveguide and the silicon waveguide.

The phase shifter uses the Pockels effect of EO polymer to achieve phase modulation. Under an appropriate synthesis and poling process, EO polymer shows great potential for high EO coefficient [19] and it is not soluble in chemicals commonly used in micro-fabrication processes [20]. As in most EO polymer based silicon-organic hybrid (SOH) modulators, the confinement capability of the dielectric waveguides is restricted by diffraction limit, and modulation efficiency is reduced due to partial distribution of mode energy in the silicon strips. In contrast, EO polymer based plasmonic modulators can obtain much better confinement and thus higher modulation efficiency. Fig. 2(c) and (e) depict electric-field distributions of an MDM waveguide and a silicon slot-waveguide, respectively. The results are obtained by finite-difference time-domain (FDTD) simulations. The refractive indices of Si, $SiO_2$ and Ag are obtained from [21]–[23], respectively. The refractive index of the polymer, $n_p$, is assumed to be 1.63 in the simulations. As shown in Fig. 2(c), in the MDM waveguide, 51.7% of the optical power is confined within the slot. However, in the silicon-slot waveguide, shown in Fig. 2(e), 16.9% of the optical power is localized inside the slot.

The modulation bandwidth of an SOH modulator is inversely proportional to the $RC$ time constant, where $R$ is the resistance of the conductive silicon strips and $C$ is the capacitance
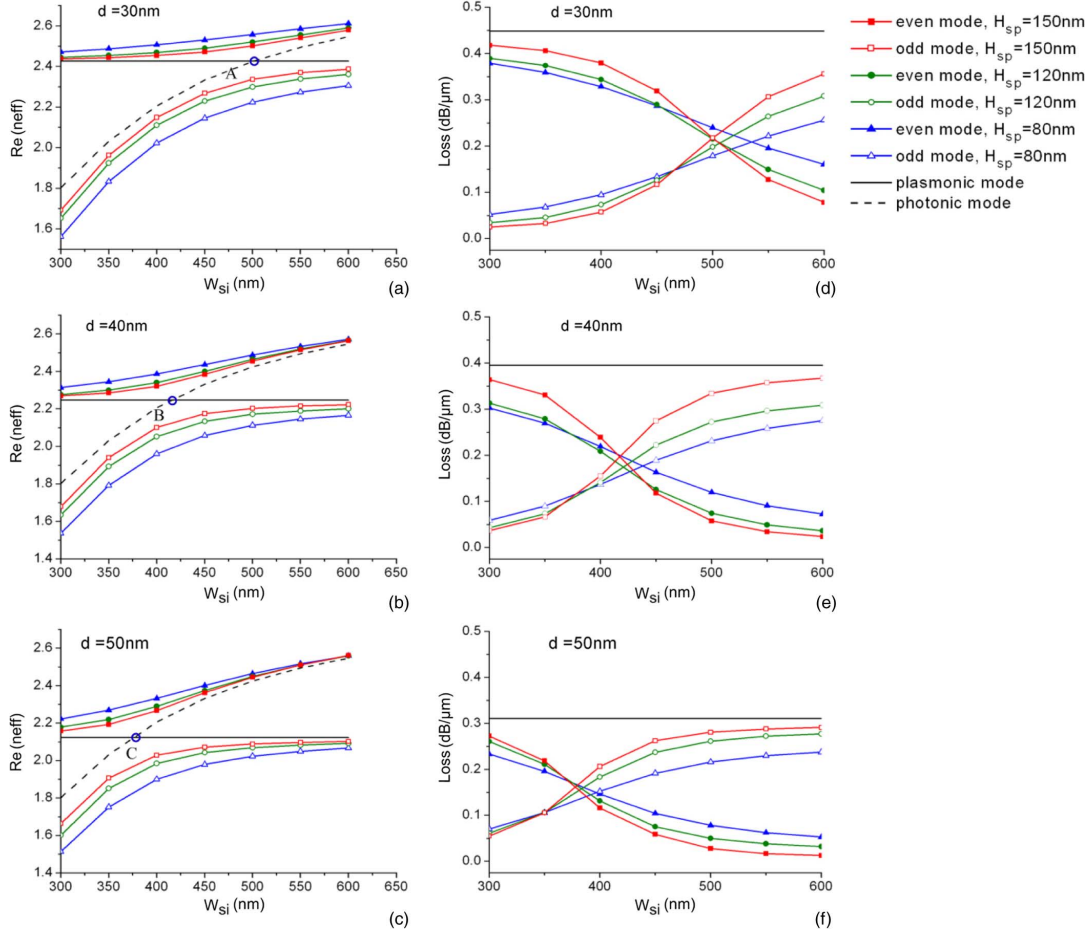
Fig. 3. (Color online) (a)–(c) Real parts of the effective indices and (d)–(f) losses of the quasi-even, quasi-odd, plasmonic, and photonic modes as a function of silicon waveguide width, for various MDM slot widths and silica-space heights. $W_{si}$: silicon waveguide width. $d$: MDM slot width. $H_{sp}$: height of the silica space between the silicon waveguide and the metal plates.

of the slot [3]. Due to a higher than expected resistance possibly caused by metal-semiconductor contacts or surface states of the silicon strips [4], [6], the $RC$ time constant is usually large, limiting the modulation bandwidth. However, in our structure, the electrical signals are directly applied to the capacitor without transmission in the doped silicon strips, thus greatly reducing the $RC$ time constant and also overcoming the limitation from free carrier effects in silicon.

### B. Mode Analysis of the Silicon-Plasmonic Hybrid Phase Shifter

The operation principle of the proposed hybrid phase shifter is similar to that in a conventional directional coupler [24]. When light is launched into the silicon-plasmonic hybrid phase shifter, the original photonic mode in Fig. 2(d), with propagation constant $\beta_d$, excites two eigenmodes shown in Fig. 2(a) and (b). The quasi-even mode is of even symmetry with complex propagation constant $\beta_e = \beta'_e + i\beta''_e$ and the quasi-odd mode is of odd symmetry with $\beta_o = \beta'_o + i\beta'_o$. Radiation modes are not considered here since they account for less than 0.5% of the total optical power, as calculated using modal decomposition method in [25]. With $n_e = n'_e + in''_e$, $n_o = n'_o + in''_o$, $n_d$, and $n_p = n'_p + in''_p$ as the complex effective indices of the quasi-even, quasi-odd, silicon waveguide, and

MDM plasmonic mode respectively, one can obtain $\beta_e = k_0 n_e$, $\beta_o = k_0 n_o$, $\beta_d = k_0 n_d$, and $\beta_p = k_0 n_p$, where $k_0 = 2\pi/\lambda$ is the vacuum propagation constant and $\beta_p = \beta'_p + i\beta''_p$ is the propagation constant of the MDM plasmonic mode. Since $\beta'_e \neq \beta'_o$, the optical power periodically transfers between the silicon and plasmonic waveguides, which is caused by the beating between the quasi-even and quasi-odd modes.

We use the coupled mode theory to estimate the transfer function of the silicon-plasmonic hybrid phase shifter [26], [27]. Let $\kappa$ and $\delta = (\beta_d - \beta'_p)/2$ denote the coupling constant and phase velocity mismatch between the silicon-waveguide photonic mode and MDM plasmonic mode respectively. Given lossy waveguides with $|n'_e - n'_o| \gg |n''_e - n''_o|$ and $\delta/\kappa \ll 1$, the transfer matrix of the hybrid phase shifter can be derived as follows [27]:

$$\begin{bmatrix} E_d(z) \\ E_p(z) \end{bmatrix} = \begin{bmatrix} A(z)e^{-z/L_p}e^{-i\beta_d z} & B(z)e^{-z/L_p}e^{-i\beta_d z} \\ -B^*(z)e^{-z/L_p}e^{-i\beta'_p z} & A^*(z)e^{-z/L_p}e^{-i\beta'_p z} \end{bmatrix}$$
$$\times \begin{bmatrix} E_d(0) \\ E_p(0) \end{bmatrix} \tag{1}$$

$$A(z) = e^{i\delta z}\left[\cos(sz) - i\frac{\delta}{s}\sin(sz)\right] \tag{2}$$

$$B(z) = -ie^{i\delta z}\frac{\kappa}{s}\sin(sz) \tag{3}$$

where $E_d(z)$ or $E_p(z)$ is the electric field concentrated on the silicon waveguide or MDM slotline consisting the hybrid phase shifter respectively, $s = \sqrt{|\kappa|^2 + |\delta|^2}$, and $L_p = 2/\beta_p''$ is the mean attenuation length of the hybrid waveguide, which is defined as the distance that the amplitude of the field attenuates to 1/e. From (1) to (3), given $E_p(0) = 0$, the fraction of optical power coupled from the silicon waveguide to the MDM waveguide can be expressed as

$$\eta(z) = \frac{|E_p(z)|^2}{|E_d(0)|^2} = e^{-2z/L_p}|B(z)|^2 = Fe^{-2z/L_p}\sin^2\left(\frac{\pi z}{2L_c}\right) \quad (4)$$

where $F = |\kappa|^2/s^2$ is the maximum fraction of coupled optical power, $L_c = \pi/(2s)$ is the coupling length. Under the strong coupling conditions that $\delta \approx 0$ and $\delta/\kappa \ll 1$, $\kappa$ can be simplified as $(\beta_e' - \beta_o')/2$ [24], then

$$L_c \approx \frac{\pi}{2|\kappa|} = \frac{\pi}{|\beta_e' - \beta_o'|} = \frac{\lambda}{2|n_e' - n_o'|} \quad (5)$$

and $F \approx 1$, which improves the modulation efficiency of the hybrid phase shifter by increasing the fraction of optical power periodically coupled into the MDM slotline filled with EO polymer.

Several factors should be considered in choosing the dimensions of the silicon-plasmonic hybrid phase shifter. Fig. 3 shows the real parts of the effective indices and the losses for the quasi-even, quasi-odd, plasmonic, and photonic modes as the silicon waveguide width $W_{si}$ decreases from 600 nm to 300 nm. From (4), in order to get a high coupling efficiency, the phase velocities of silicon-waveguide photonic mode and MDM plasmonic mode should be matched, which requires $\delta \approx 0$ as marked by the points A to C in Fig. 3(a) to (c), respectively. Propagation loss is also an important factor for the design of a plasmonic device. As shown in Fig. 3(d) to (f), when silicon waveguide width is reduced, the propagation loss of the quasi-even mode and quasi-odd mode increases and decreases, respectively. Meanwhile, with a larger slot width, the loss of the MDM plasmonic mode becomes smaller, which, on the other hand, could reduce the modulation efficiency of the phase shifter by weakening the applied electric field inside the slot. Integrating the factors including phase match, propagation loss, modulation efficiency, and fabrication feasibility, the dimensions of the silicon waveguide are set to 370 nm (width) and 220 nm (height). The MDM waveguide is 120 nm above the silicon waveguide with a 50-nm-wide and 100-nm-high slot. These device geometric parameters will be used in the following discussions.

Fig. 4 depicts the distributions of optical energy density propagating along the silicon waveguide and MDM waveguide of the hybrid phase shifter with a length of $4L_c$, which are achieved by three-dimensional FDTD method. The interference pattern is induced by the beating between the quasi-even and quasi-odd modes. When the strong coupling conditions are satisfied as shown in Fig. 4(a), a nearly complete periodic power transfer between the photonic mode and plasmonic mode takes place. Simulations show that the coupling length is 2.4 $\mu$m and 68% of the incident power is transmitted to the output silicon waveguide. However, as shown in Fig. 4(b), when the silicon
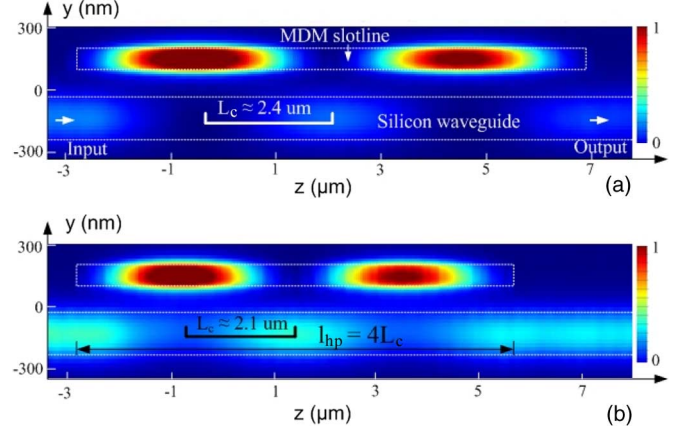


Fig. 4. (Color online) Electromagnetic energy density distributions simulated by three-dimensional FDTD method for the proposed silicon-plasmonic hybrid phase shifter with (a) 370-nm silicon waveguide width and 9.7-$\mu$m hybrid waveguide length, and (b) 420-nm silicon waveguide width and 8.5-$\mu$m hybrid waveguide length. Other geometrical dimensions are: $d = 50$ nm, $H_{slot} = 100$ nm, $H_{sp} = 120$ nm, and $H_{si} = 220$ nm.

waveguide width increases to 420 nm with other simulation parameters unchanged, $L_c$ is reduced to 2.1 $\mu$m. Due to a larger phase mismatch between the photonic mode and plasmonic mode, strong coupling conditions are not satisfied and only part of the optical power can be coupled from the silicon waveguide to the MDM waveguide.

### C. Design of the Silicon Racetrack Ring Modulator

After the light is launched into the hybrid phase shifter, using (1) and given $E_p(0) = 0$, one can obtain the transmission function of the hybrid phase shifter as

$$T_{hp} = \frac{E_d(l_{hp})}{E_d(0)} = e^{-l_{hp}/L_p}e^{-i(\beta_d-\delta)l_{hp}}$$
$$\times [\cos(sl_{hp}) - i(\delta/s)\sin(sl_{hp})] \quad (6)$$

After the hybrid phase shifter is integrated with the racetrack ring structure as shown in Fig. 1(a), the transmission function of the ring modulator can be derived by the multiple round-trip approach [28]:

$$T = \frac{E_{out}}{E_{in}} = \frac{t - \alpha T_{hp}e^{-i\beta_d(l-l_{hp})}}{1 - \alpha t T_{hp}e^{-i\beta_d(l-l_{hp})}} \quad (7)$$

where $E_{in}/E_{out}$ is the input/output electric field of the bus waveguide respectively, $t$ is the transmission coefficient between the ring and the bus waveguide, $l$ is the circumference of the ring resonator, and $\alpha$ is the round-trip loss factor of the silicon waveguide section in the racetrack resonator including bending loss and waveguide loss [29]. Based on (6), the optical energy should completely transfer to the silicon waveguide at the end of the hybrid phase shifter, which requires:

$$sl_{hp} = m_1\pi \quad (8)$$

where $m_1$ is a positive integer. The on-resonance condition of the racetrack ring can be derived from (7):

$$\beta_d l - \delta l_{hp} = 2m_2\pi \quad (9)$$

where $m_2$ is a positive integer.
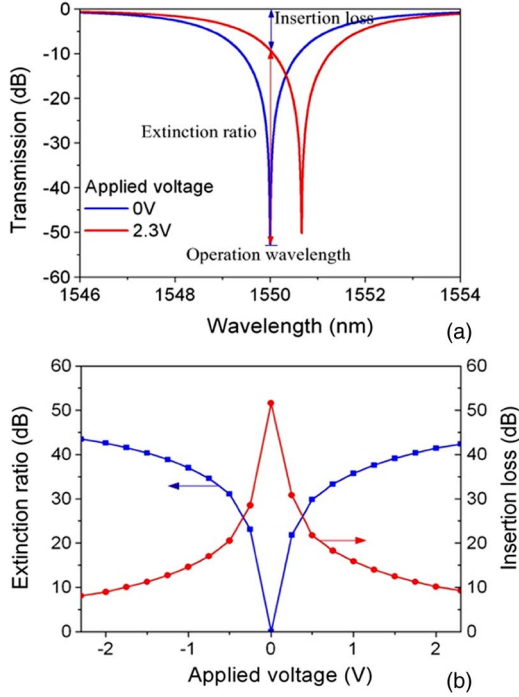
Fig. 5.  (Color online) (a) Transmission spectra of the proposed modulator under 0-V and 2.3-V DC bias voltages across the MDM slot. Maximum extinction ratio, corresponding insertion loss and operation wavelength are shown. (b) Extinction ratio and insertion loss under various applied voltages from −2.3 V to +2.3 V.

The transmission coefficient $t$ can be adjusted to obtain a quasi-critical coupling in order to achieve a high resonance extinction ratio. Fig. 5(a) provides the spectra of the proposed modulator with the resonances around 1550 nm. The spectra are obtained from (7) and the corresponding parameters of the modulator are: $W_{si} = 370$ nm, $H_{si} = 220$ nm, $H_{sp} = 120$ nm, $d = 50$ nm, $H_{slot} = 100$ nm, $l = 34.3$ $\mu$m, $l_{hp} = 9.52$ $\mu$m, $L_p = 52.12$ $\mu$m, $\alpha = 0.98$, and $t = 0.836$. The effective refractive indices at 0-V bias are: $n'_e = 2.2458$, $n'_o = 1.9201$, $n_d = 2.1247$, and $n'_p = 2.1244$, which are obtained from FDTD simulations.

## D. Modulation Analysis, High-Speed Characteristic, and Low Energy Consumption

After the deposition of EO polymer over the MDM waveguide and an efficient poling process, the EO polymer may achieve a high EO coefficient, $\gamma_{33}$, of 50–300 pm/V at the wavelength of 1550 nm [30]. For the proposed modulator, $\gamma_{33}$ is assumed to be 80 pm/V. Considering that the EO polymer typically has a very high resistivity of more than $10^{11}$ $\Omega \cdot$ cm [17], the two parallel metal plates of the MDM waveguide are electrically isolated and can be used as the modulator electrodes. The refractive index variation of the polymer inside the slot under an applied voltage, $V$, can be expressed as

$$\Delta n = \frac{1}{2}n_p^3 \gamma_{33} \frac{V}{d}. \tag{10}$$

The phase-modulation speed is intrinsically very high due to the fast response of the Pockels effect. With the ring resonator,

the phase modulation is converted into intensity modulation by shifting the transmission curve. Supposing that the refractive index of the EO polymer can increase and decrease under positive and negative biases, then the resonance experiences a red-shift and a blue-shift, respectively [31]. Fig. 5(a) defines the extinction ratio and insertion loss of the modulator with operation wavelength fixed at 1550 nm. As shown in Fig. 5(b), an increased bias voltage results in a larger resonance shift thus leading to an increased extinction ratio and a decreased insertion loss. An extinction ratio of more than 30 dB is achieved when $|V| > 1$ V and the polymer refractive index change is within $8 \times 10^{-3}$ when the bias voltage across the MDM slot varies from $-2.3$ V to $+2.3$ V.

The modulation bandwidth of a ring modulator is limited by factors including $RC$ time constant, photon life time, and driver electronics. One of the attractive features for the proposed modulator is the potential for high modulation speed due to its small $RC$ time constant and short photon life time. The two parallel metal plates with the EO polymer sandwiched in between form a capacitor. The capacitance can be estimated by $C_m = \varepsilon_0 \varepsilon_r A/d \approx 0.4$ fF, where $\varepsilon_0$ is the permittivity of vacuum, $\varepsilon_r = 2.657$ is the dielectric constant of EO polymer, and $A$ is the sidewall area of the metal plates. Due to its compact size, the modulator can be regarded as a lumped element with no need for travelling-wave electrode design. The $RC$-limited 3-dB bandwidth of the modulator is proportional to $1/R_m C_m$, where $R_m$ is the loading resistance depending on the electrode layout and fabrication processes. A typical value of $R_m$ is 50 $\Omega$ [10] and thus $1/R_m C_m$ is calculated on the order of terahertz, which is not considered as a major limitation on the modulation speed. As the metal plates can be used as electrodes to conduct electrical signals directly to the active polymer, the $RC$ time constant is reasonably much smaller than that induced by free carrier transit in silicon, thus leading to an increased modulation bandwidth.

On the other hand, in the optical regime, the photon life time in the ring resonator $\tau_r$ sets a fundamental limit to the modulation speed. $\tau_r$ can be obtained from the quality factor of the ring, $Q_r$, as [8]

$$\tau_r = \frac{Q_r \lambda}{2\pi c} \tag{11}$$

$$Q_r = \frac{\lambda_0}{\Delta\lambda} \tag{12}$$

where $\lambda_0$ and $\Delta\lambda$ are the central wavelength and the 3-dB bandwidth of the resonance respectively. Due to the intrinsic loss induced by the MDM plasmonic waveguide, a decreased quality factor can be obtained for the racetrack ring with the hybrid phase shifter. As shown in Fig. 5(a), $\Delta\lambda$ of the proposed modulator at 1550 nm is ~3.6 nm corresponding to $Q_r \approx 430$. Thus, from (11), the photon life time in the proposed modulator is 0.35 ps, corresponding to a bandwidth larger than 300 GHz, exceeding the performance of existing silicon ring modulators.

The power consumption can be estimated by $P = C_m V^2 f/2$ [10], where $V$ is the voltage amplitude and $f$ is the modulation frequency. Given $V$ of 2.3 V, $P$ is on the order of $10^{-1}$ mW at a modulation frequency up to 100 GHz. Thus, without fundamental limitation on bandwidth from electro-optic response,
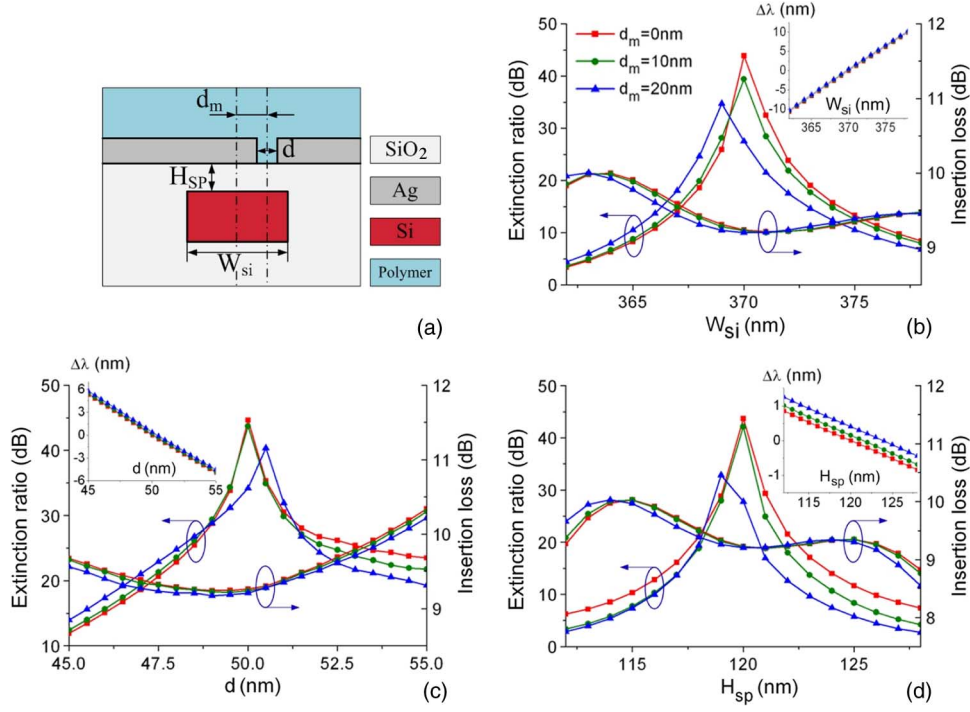
Fig. 6. (Color online) Modulator performances including extinction ratio, insertion loss, and resonance shift of the proposed modulator when fabrication errors and structural mismatches in geometrical dimensions labeled in (a) are taken into consideration. These geometrical dimensions include (b) silicon waveguide width, $W_{si}$, varying from 362 nm to 378 nm, (c) MDM slot width, $d$, varying from 45 nm to 55 nm, and (d) height of the silica space, $H_{sp}$, varying from 112 nm to 128 nm. $d_m$ is defined as the distance between the silicon and the MDM waveguide centers. A positive or negative $\Delta\lambda$ corresponds to a red or blue shift of the resonance, respectively.

$RC$ time constant, and optical resonance, such an energy-efficient modulator can be used in future SOI photonic circuits to build high-speed low-power-consumption inter-chip optical interconnects and also terabit per channel optical communication links.

## III. TOLERANCE TO FABRICATION ERRORS AND MISMATCHES

Since the silicon-plasmonic hybrid modulator operation is based on a resonator system under the phase matching conditions described in (8) and (9), it is essential to consider the performance tolerance to fabrication errors and mismatches, especially those induced by the hybrid phase shifter which plays a key role in mode confinement and phase modulation process. Fabrication errors and mismatches in silicon-waveguide width, MDM slot width, silica-space height, and lateral alignment are considered here as shown in Fig. 6(a). Their influences on extinction ratio, insertion loss, and resonant wavelength are depicted in Fig. 6(b) to (d). The extinction ratio and insertion loss are achieved when the bias voltage across the MDM slot changes from 0 V to 2.3 V. The proposed racetrack resonator initially satisfies critical coupling condition defined as

$$t = a|T_{hp}|. \tag{13}$$

Using (6) and (7), one can derive the intensity of $T_{hp}$ and the round-trip phase accumulated in the racetrack resonator, $\phi$, as follows:

$$|T_{hp}|^2 = e^{-2l_{hp}/L_p}\left[\cos^2(sl_{hp}) + \left(\frac{\delta}{s}\right)^2\sin^2(sl_{hp})\right] \tag{14}$$

$$\phi \approx \beta_d l - \delta l_{hp}. \tag{15}$$

When the widths of the silicon waveguide and MDM slot change within a small range, e.g., $\pm 8$ nm and $\pm 5$ nm, respectively, the coupling constant $\kappa$ keeps almost the same, the phase velocity mismatch $|\delta|$ increases, leading to a larger $s$ in (14). Then the transmission, $|T_{hp}|$, is decreased. The resonator will operate in under-coupling regime defined as $t > a|T_{hp}|$. Consequently, the resonance depth degrades, leading to a reduced extinction ratio as shown in Fig. 6(b) and (c). Similarly, the uncertainty of silica-space height and the misalignment between the silicon and plasmonic waveguides can also reduce $|T_{hp}|$, thus leading to an under-coupled resonator with a decreased extinction ratio as shown in Fig. 6(b) to (d). However, the resonance shift is relatively small in the inset of Fig. 6(d) because, from FDTD simulation results, both $\beta_d$ and $\delta$ are relatively insensitive to the change of silica-space height and therefore leading to an insignificant phase shift in (15).

The extinction ratio is quite sensitive to fabrication errors, especially those of the silicon waveguide width and silica-space height as shown in Fig. 6(b) and (d) respectively. Such errors may be reduced with the state-of-the-art nano-fabrication technologies [32], [33] to control the dimension variance within a reasonable range. The resonance shift can also be corrected to some extent by thermal tuning the refractive index of the straight waveguide section in the racetrack ring modulator. One possible scheme to insert the thermal heater is provided in [34]. Compared with the extinction ratio, the insertion loss that changes around 9 dB to 10 dB is relatively insensitive to the fabrication errors as shown in Fig. 6(b) to (d).

## IV. FABRICATION FEASIBILITY

The proposed modulator could be realized by the following nano-fabrication steps demonstrated in [4], [32], [35]. Firstly, electron beam lithography (EBL) is used to pattern the photoresist on an SOI wafer, with a 220-nm silicon layer and 3-$\mu$m buried oxide. The photoresist pattern then acts as a mask for the following dry etching of the silicon to form the racetrack ring and the bus waveguide with an etch depth of 220 nm. Secondly, after the device is clad with 120-nm-thick silicon oxide, another photoresist layer is spun and an EBL step is performed to open the window for metal evaporation. A 100-nm-thick silver film is evaporated onto the chip followed by a lift-off process. Focused-ion-beam (FIB) is used to obtain a 50-nm-wide slot inside the silver layer. Silver is used here because it has a relatively small absorption loss at the wavelength of 1550 nm. Thirdly, the EO polymer cladding is prepared by spin-coating. Here, we assume that the polymer can enter the 50-nm-wide slot, which is confirmed by [36]. One may need to adjust the width of the slot to guarantee the polymer filling in the gap and subsequently change the dimensions of the hybrid phase shifter using the aforementioned analytical method. In order to achieve a high EO coefficient inside the slot, the polymer should be properly poled before device operation, which requires a large electric field applied to the two parallel metal plates.

## V. CONCLUSION

In this paper, an electro-optic modulator based on a silicon-plasmonic hybrid phase shifter is proposed. The modulator is composed of two layers with the bottom one comprising a silicon racetrack ring coupled to a bus waveguide, and the top layer formed by an MDM plasmonic-slot waveguide, which aligns with one of the straight waveguide sections of the ring resonator. The slot is filled with EO polymer to enable electro-optic modulation. Due to an ultrafast response speed of the Pockels effect, a compact size, a reduced $RC$ delay, and a decreased quality factor of the ring, the proposed modulator shows the prospect to achieve an ultrahigh modulation speed and a low energy consumption. The effects of the fabrication errors and mismatches on the performance of the proposed modulator are also investigated. Such an electro-optic modulator based on the silicon-plasmonic hybrid phase shifter is promising for applications in future silicon inter-chip interconnects or ultrahigh-speed optical communication networks.

## REFERENCES

[1] F. Y. Gardes, D. J. Thomason, N. G. Emerson, and G. T. Reed, "40 Gb/s silicon photonics modulator for TE and TM polarisations," *Opt. Exp.*, vol. 19, no. 12, pp. 11804–11814, Jun. 2011.

[2] G. T. Reed, G. Mashanovich, F. Y. Gardes, and D. J. Thomson, "Silicon optical modulators," *Nature Photon.*, vol. 4, pp. 518–526, Jul. 2010.

[3] L. Alloatti, D. Korn, R. Palmer, D. Hillerkuss, J. Li, A. Barklund, R. Dinu, J. Wieland, M. Fournier, J. Fedeli, H. Yu, W. Bogaerts, P. Dumon, R. Baets, C. Koos, W. Freude, and J. Leuthold, "42.7 Gbit/s electro-optic modulator in silicon technology," *Opt. Exp.*, vol. 19, no. 12, pp. 11841–11851, Jun. 2011.

[4] R. Ding, T. B. Jones, Y. Liu, R. Bojko, J. Witzens, S. Huang, J. Luo, S. Benight, P. Sullivan, J.-M. Fedeli, M. Fournier, L. Dalton, A. K.-Y. Jen, and M. Hochberg, "Demonstration of a low $V_\pi L$ modulator with GHz bandwidth based on electro-optic polymer-clad silicon slot waveguides," *Opt. Exp.*, vol. 18, no. 15, pp. 15618–15623, Jul. 2010.

[5] Y. Tang, H.-W. Chen, S. Jain, J. D. Peters, U. Westergren, and J. E. Bowers, "50 Gb/s hybrid silicon traveling-wave electroabsorption modulator," *Opt. Exp.*, vol. 19, no. 7, pp. 5811–5816, Mar. 2011.

[6] T. B. Jones, B. Penkov, J. Huang, P. Sullivan, J. Davies, J. Takayesu, J. Luo, T.-D. Kim, L. Dalton, A. K.-Y. Jen, M. Hochberg, and A. Scherer, "Nonlinear polymer-clad silicon slot waveguide modulator with a half wave voltage of 0.25 V," *Appl. Phys. Lett.*, vol. 92, no. 16, Apr. 2008.

[7] J. Ding, H. Chen, L. Yang, L. Zhang, R. Ji, Y. Tian, W. Zhu, Y. Lu, P. Zhou, and R. Min, "Low-voltage, high-extinction-ratio, Mach-Zehnder silicon optical modulator for CMOS-compatible integration," *Opt. Exp.*, vol. 20, no. 3, pp. 3209–3218, Jan. 2012.

[8] Q. Xu, V. R. Almeida, and M. Lipson, "Micrometer-scale all-optical wavelength converter on silicon," *Opt. Lett.*, vol. 30, no. 20, pp. 2733–2735, Oct. 2005.

[9] S. I. Inoue and S. Yokoyama, "Numerical simulation of ultra-compact electro-optic modulator based on nanoscale plasmon metal gap waveuides," *Electron. Lett.*, vol. 45, no. 21, pp. 1087–1089, Oct. 2009.

[10] W. Cai, J. S. White, and M. L. Brongersma, "Compact, high-speed and power-efficient electrooptic plasmonic modulators," *Nano Lett.*, vol. 9, no. 12, pp. 4403–4411, Oct. 2009.

[11] J. A. Dionne, L. A. Sweatlock, and H. A. Atwater, "Plasmon slot waveguides: Towards chip-scale propagation with subwavelength-scale localization," *Phys. Rev. B*, vol. 73, no. 3, Jan. 2006.

[12] S. Zhu, G. Q. Lo, and D. L. Kwong, "Electro-absorption modulation in horizontal metal-insulator-silicon-insulator-metal nanoplasmonic slot waveguides," *Appl. Phys. Lett.*, vol. 99, no. 15, Oct. 2011.

[13] A. Melikyan, N. Lindenmann, S. Walheim, P. Leufke, S. Ulrich, J. Ye, P. Vincze, H. Hahn, T. Schimmel, and C. Koos, "Surface plasmon polariton absorption modulator," *Opt. Exp.*, vol. 19, no. 9, pp. 8855–8869, Apr. 2011.

[14] V. J. Sorger, N. D. Lanzillotti-Kimura, R. M. Ma, and X. Zhang, "Ultra-compact silicon nanophotonic modulator with broadband response," *Nanophotonics*, vol. 1, no. 1, pp. 17–22, Jul. 2012.

[15] J. A. Dionne, L. A. Sweatlock, M. T. Sheldon, A. P. Alivisatos, and H. A. Atwater, "Silicon-based plasmonics for on-chip photonics," *IEEE J. Sel. Topics Quantum Electron.*, vol. 16, no. 1, pp. 295–306, Jan. 2010.

[16] S. Zhu, G. Q. Lo, and D. L. Kwong, "Theoretical investigation of silicon MOS-type plasmonic slot waveguide based MZI modulators," *Opt. Exp.*, vol. 18, no. 26, pp. 27802–27819, Dec. 2010.

[17] X. Sun, L. Zhou, X. Li, Z. Hong, and J. Chen, "Design and analysis of a phase modulator based on a metal-polymer-silicon hybrid plasmonic waveguide," *Appl. Opt.*, vol. 50, no. 20, pp. 3428–3434, Jul. 2011.

[18] B. Bortnik, Y.-C. Hung, H. Tazawa, B. J. Seo, J. Luo, A. K.-Y. Jen, W. H. Steier, and H. R. Fetterman, "Electrooptic polymer ring resonator modulation up to 165 GHz," *IEEE J. Sel. Topics Quantum Electron.*, vol. 13, no. 1, pp. 104–110, Feb. 2007.

[19] J. Luo, X.-H. Zhou, and A. K.-Y. Jen, "Rational molecular design and supramolecular assembly of highly efficient organic electro-optic materials," *J. Mater. Chem.*, vol. 19, pp. 7410–7424, Aug. 2009.

[20] H. Sun, A. Pyajt, J. Luo, Z. Shi, S. Hau, A. K.-Y. Jen, L. R. Dalton, and A. Chen, "All-dielectric electrooptic sensor based on a polymer microresonator coupled side-polished optical fiber," *IEEE Sensors J.*, vol. 7, no. 4, pp. 515–524, Apr. 2007.

[21] E. D. Palik, *Handbook of Optical Constants of Solids*. Orlando, FL, USA: Academic, 1985, pp. 558–569.

[22] E. D. Palik, *Handbook of Optical Constants of Solids*. Orlando, FL, USA: Academic, 1985, pp. 753–763.

[23] P. B. Johnson and R. W. Christy, "Optical constants of the noble metals," *Phys. Rev. B*, vol. 6, no. 12, pp. 4370–4379, Dec. 1972.

[24] Q. Li and M. Qiu, "Structurally-tolerant vertical directional coupling between metal-insulator-metal plasmonic waveguide and silicon dielectric waveguide," *Opt. Exp.*, vol. 18, no. 15, pp. 15531–15543, Jul. 2010.

[25] Q. Li, Y. Song, G. Zhou, Y. Su, and M. Qiu, "Asymmetric plasmonic-dielectric coupler with short coupling length, high extinction ratio, low insertion loss," *Opt. Lett.*, vol. 35, no. 19, pp. 3153–3155, Oct. 2010.

[26] C. Delacour, S. Blaize, P. Grosse, J. M. Fedeli, A. Bruyant, R. S. Montiel, G. Lerondel, and A. Chelnokov, "Efficient directional coupling between silicon and copper plasmonic nanoslot waveguides: Toward metal-oxide-silicon nanophotonics," *Nano Lett.*, vol. 10, no. 8, pp. 2922–2926, Jul. 2010.

[27] A. Yariv and P. Yeh, *Photonics: Optical Electronics in Modern Communications*, 6th ed. Oxford, U.K.: Oxford Univ. Press, Jan. 2006, ch. 13.

[28] H. Tazawa and W. H. Steier, "Analysis of ring resonator-based traveling-wave modulators," *IEEE Photon. Technol. Lett.*, vol. 18, no. 1, pp. 211–213, Jan. 2006.

[29] P. Dong, S. F. Preble, and M. Lipson, "All-optical compact silicon comb switch," *Opt. Exp.*, vol. 15, no. 15, pp. 9600–9605, Jul. 2007.

[30] R. Ding, T. B. Jones, W.-J. Kim, A. Spott, M. Fournier, J.-M. Fedeli, S. Huang, J. Luo, A. K.-Y. Jen, L. Dalton, and M. Hochberg, "Sub-volt silicon-organic electro-optic modulator with 500 MHz bandwidth," *J. Lightw. Technol.*, vol. 29, no. 8, pp. 1112–1117, Apr. 2011.

[31] M. Gould, T. B. Jones, R. Ding, S. Huang, J. Luo, A. K.-Y. Jen, J.-M. Fedeli, M. Fournier, and M. Hochberg, "Silicon-polymer hybrid slot waveguide ring-resonator modulator," *Opt. Exp.*, vol. 19, no. 5, pp. 3952–3961, Feb. 2011.

[32] J. Tian, S. Yu, W. Yan, and M. Qiu, "Broadband high-efficiency surface-plasmon-polariton coupler with silicon-metal interface," *Appl. Phys. Lett.*, vol. 95, no. 1, Jul. 2009.

[33] S. Zhu, T. Liow, G. Lo, and D. Kwong, "Silicon-based horizontal nanoplasmonic slot waveguides for on-chip integration," *Opt. Exp.*, vol. 19, no. 9, pp. 8888–8902, 2011.

[34] T. Wang, M. Xu, F. Li, J. Wu, L. Zhou, and Y. Su, "Design of high-modulation-depth, low-energy silicon modulator based on coupling tuning in a resonance-split microring," *J. Opt. Soc. Amer. B*, vol. 29, no. 11, pp. 3047–3055, Nov. 2012.

[35] B. Guha, B. B. C. Kyotoku, and M. Lipson, "CMOS-compatible athermal silicon microring resonators," *Opt. Exp.*, vol. 18, no. 4, pp. 3487–3493, Feb. 2010.

[36] M. Hochberg, T. B. Jones, G. Wang, J. Huang, P. Sullivan, L. Dalton, and A. Scherer, "Towards a millivolt optical modulator with nano-slot waveguides," *Opt. Exp.*, vol. 15, no. 13, pp. 8401–8410, Jun. 2007.

**Mu Xu** received the B.S. degree in electronics engineering in 2010 from Department of Sophisticated Instruments and Optoelectronics Engineering, Tianjin University, Tianjin, China. He is currently a graduate student in communication engineering at Shanghai Jiao Tong University, Shanghai, China.

His current research interests include silicon photonics, plasmonic photonics and optical signal processing on silicon chips.

**Fei Li** received the B.S. degree in 2010 from Ocean University of China, Qingdao, China. She is currently a graduate student in communication engineering at Shanghai Jiao Tong University, Shanghai, China.

Her current research interests include silicon photonics and optical plasmonics, as well as integrated passive and active devices.

**Tao Wang** (SM'08) received the B.S. degree in electronics engineering from the Department of Electronic Engineering, Shandong University, China, in 2004, and the M.S. degree from the graduate school of the Chinese Academy of Sciences, Beijing, China, in 2007. He is currently pursuing the Ph.D. degree at Shanghai Jiao Tong University, Shanghai, China.

His current research interests include microwave photonics and information processing in silicon waveguides.

**Jiayang Wu** received the B.S. degree in communication engineering in 2010 from Xidian University, Xian, China. He is currently pursuing the Ph.D. degree at Shanghai Jiao Tong University, Shanghai, China.

His current research interests include silicon photonics and micro-fabrication technologies of photonic devices.

**Liyang Lu** received the B.S. degree in information engineering from Shanghai Jiao Tong University, Shanghai, China, in 2012.

His current research interests include silicon-based photonics and surface plasmonic polaritons.

**Linjie Zhou** (M'04) received the B.S. degree in microelectronics from Peking University, Beijing, China, in 2003. He received the Ph.D. degree in electronic and computer engineering from the Hong Kong University of Science and Technology, Hong Kong, China, in 2007.

From 2007 to 2009, Dr. Zhou was a Postdoctoral Research Scientist in electrical and computer engineering at University of California, Davis, CA, USA. He is currently an Associate Professor in the State Key Lab of Advanced Optical Communication Systems and Networks in Shanghai Jiao Tong University, Shanghai, China. His research interests include silicon micro/nano optical devices and their integration for optical communication and interconnect applications. He has been the author or co-author of nearly 50 journal articles and conference papers.

**Yikai Su** (S'97–M'01–SM'07) received the B.S. degree from the Hefei University of Technology, Hefei, China, in 1991, the M.S. degree from the Beijing University of Aeronautics and Astronautics, Beijing, China, in 1994, and the Ph.D. degree in electronics engineering from Northwestern University, Evanston, IL, in 2001.

He was with Crawford Hill Laboratory of Bell Laboratories for three years before he joined the Shanghai Jiao Tong University, Shanghai, China, as a Full Professor in 2004. His current research interests include modulation formats, and micro/nano photonic devices for information processing. He has been the author or co-author of more than 200 journal articles and conference papers.

Prof. Su is a member of the Optical Society of America. He is a Topical Editor of *Optics Letters*, Guest Editor of IEEE JOURNAL OF SELECTED TOPICS ON LIGHTWAVE TECHNOLOGY on "Nonlinear Optical Signal Processing" in 2008/2011, and a Feature Editor of Applied Optics on the special issue of AOE 2008. He serves as a TPC member of OFC (2011–2013) and ECOC (2013–), and is the chapter chair of IEEE Photonics Society in Shanghai, China.